Utilizing Walrus Optimizer with Chaotic Maps for Solving Engineering Design Optimization Problems

Pasura Aungkulanon
Department of Materials Handling and Logistics Engineering, Faculty of Engineering, King Mongkut's University of Technology North Bangkok, Bangkok, Thailand
pasura.a@eng.kmutnb.ac.th

Lakkana Ruekkasaem
Department of Mathematics and Statistics, Faculty of Science and Technology, Thammasat University, Pathumthani, Thailand
lakkana@mathstat.sci.tu.ac.th (corresponding author)

Pongchanun Luangpaiboon
Department of Industrial Engineering, Faculty of Engineering, Industrial Statistics and Operational Research Unit (ISO-RU), Thammasat School of Engineering, Thammasat University, Pathumthani, Thailand
lpongch@engr.tu.ac.th (corresponding author)

Received: 28 August 2025 | Revised: 18 September 2025 | Accepted: 6 October 2025

 DOI: https://doi.org/10.48084/etasr.14367

ABSTRACT

Modern manufacturing is significantly influenced by machining optimization, which enhances surface quality, reduces production costs, and improves material removal efficiency. However, conventional optimization methods often struggle with the nonlinear, multi-constrained nature of machining problems. Metaheuristic algorithms have emerged as effective alternatives, and the Walrus Optimizer (WO) is a recent bio-inspired method that models walrus behaviors, such as migration, breeding, and foraging. Despite its promising structure, the original WO suffers from premature convergence and limited search diversity due to its reliance on uniform random numbers. To address these shortcomings, this study proposes a hybrid framework that integrates the chaos theory into WO by embedding three chaotic maps—Logistic, Chebyshev, and Iterative Chaotic Map with Infinite Collapses (ICMIC)—into the initialization, migration, reproduction, and foraging phases. These chaos-enhanced variants, namely WO-Logistic, WO-Chebyshev, and WO-ICMIC, are applied to four benchmark machining optimization problems: (1) surface roughness minimization, (2) Material Removal Rate (MRR) maximization, (3) multi-pass turning cost minimization, and (4) a multi-objective model combining time, cost, and roughness. Comparative experiments demonstrate that the chaotic WO algorithms consistently outperform the standard WO and several state-of-the-art metaheuristics in terms of solution accuracy, convergence speed, and stability. The main contribution of this work lies in establishing a robust hybrid optimization framework that leverages the chaos theory to improve the exploration–exploitation balance. The findings highlight the potential of Chaos-enhanced Walrus Optimizer (CWO) as a reliable and generalizable tool for solving complex machining optimization problems and advancing intelligent manufacturing.

Keywords-Walrus Optimizer; chaotic map integration; hybrid metaheuristic algorithm; machining optimization; surface roughness minimization

I. INTRODUCTION

Machining optimization is a fundamental part of advanced manufacturing, with the objective of enhancing efficiency, reducing costs, and enhancing product quality. In order to achieve minimal surface roughness, maximum MRR, reduced production time, and balanced tool wear, it is imperative to select optimal parameters, including cutting speed, input rate, and depth of cut [1]. Nevertheless, the nonlinear, high-dimensional, and multimodal character of machining problems frequently restricts the use of conventional methods, including linear programming, gradient-based techniques, and exhaustive

search. As a result, metaheuristic algorithms have become increasingly popular as a result of their adaptability, robust global search capability, and derivative-free structure [2].

Numerous investigations have implemented optimization models in the context of machining [3-5]. Authors in [6] optimized three cutting parameters for multi-objective turning on a conventional lathe. Authors in [7] minimized surface roughness in Oil-Hardened Non-Shrinkable (OHNS) steel turning. Authors in [8] maximized MRR in mild steel turning. Authors in [9] proposed an enhanced differential evolution for grinding, while authors in [10] implemented simulated annealing in multi-pass turning, and authors in [11] devised a hybrid genetic–simulated annealing method. These studies substantiate the efficacy of metaheuristics in the resolution of nonlinear and constraint-heavy machining issues.

The WO is a recent bio-inspired algorithm that replicates walrus behaviors, including migration, reproduction, and foraging. Males, females, and juveniles are the three categories into which populations are divided, with each group contributing differentially to exploration and exploitation. For example, Halton sequences redistribute males to diversify exploration, adolescents utilize Lévy flights to evade predators, and females capitalize on promising regions under the influence of their leaders and mates. The equilibrium between exploration and exploitation is maintained by dynamic safety and hazard signals [10]. Although WO is adaptable, it is significantly reliant on uniform random numbers, which can limit diversity, induce premature convergence, and diminish effectiveness in multimodal search spaces.

However, the chaos theory provides an alternative to these constraints. Logistic, Chebyshev, and ICMIC are examples of chaotic maps that produce deterministic yet non-repetitive sequences that are highly sensitive to initial conditions and exhibit strong ergodicity [12]. Authors in [11] devised a hybrid genetic-simulated annealing method to concurrently enhance surface quality and decrease production time. A variety of optimization frameworks have incorporated these chaotic maps. For instance, authors in [13] proposed a Chaotic Henry Gas Solubility Optimization (CHGSO) algorithm, which was shown to have enhanced robustness and convergence in engineering design problems. Authors in [14] developed a chaotic Marine Predators Algorithm that outperformed baseline algorithms in real-world scenarios. Additionally, logistic and iterative chaotic maps have been employed to improve the search variability of the Lightning Search Algorithm [15].

The results indicate that chaos-embedded algorithms exhibit superior robustness, improved solution quality, and faster convergence in comparison to their baseline counterparts. However, no prior research has incorporated pandemonium into the WO. Furthermore, most research relies on a single chaotic map and incorporates it into only one stage of the algorithm, thereby leaving systematic multi-map, multi-phase integration largely unexplored.

This study proposes a CWO that integrates three chaotic maps—Logistic, Chebyshev, and ICMIC—into various phases of WO, such as initialization, migration, reproduction, and foraging, in order to resolve this gap. CWO improves convergence stability, exploration–exploitation balance, and population diversity by substituting random variables with chaotic sequences. The four machining benchmarks—(1) surface roughness minimization, (2) MRR maximization, (3) multi-pass turning cost minimization, and (4) a comprehensive multi-objective model that integrates time, cost, and roughness—are used to validate the proposed variants (WO-Logistic, WO-Chebyshev, WO-ICMIC).

The contributions of this study are:

- Providing experimental evidence that chaotic integration significantly enhances computational efficiency, robustness, and convergence.
- Developing three CWO variants.
- Conducting a comparative evaluation on four realistic machining models.
- Introducing a systematic multi-map, multi-phase hybridization strategy that distinguishes this work from prior chaos-enhanced metaheuristics.

Specifically, this is the initial endeavor to incorporate ICMIC into WO and the first to embed chaos across all fundamental phases of the algorithm, thereby establishing a novel framework for machining optimization.

II. RELATED METHODS

A diverse array of population-based algorithms that are capable of resolving complex, nonlinear, and multimodal optimization problems has been developed as a result of advancements in nature-inspired metaheuristics. Among these, swarm intelligence approaches have garnered particular attention for their capacity to maintain a balance between global exploration and local exploitation without employing gradient information. Nevertheless, the majority of metaheuristics encounter common challenges, including premature convergence, loss of diversity, and sensitivity to parameter settings, particularly when confronted with high-dimensional search spaces, despite their success in engineering, machine learning, and combinatorial optimization.

A plausible approach to circumventing these constraints is to combine established metaheuristics with mechanisms that can enhance search dynamics. One such mechanism is the chaos theory, which introduces deterministic, yet ergodic and aperiodic sequences that improve the coverage of the search space and the diversity of the population. The integration of chaotic maps into metaheuristic components, including initialization, parameter control, and movement operators, has been demonstrated to enhance the robustness and reliability of convergence [16]. The chaos theory serves as the diversity-enhancing mechanism in this context, while the WO serves as the baseline search framework. The proposed hybridization seeks to combine their strengths for superior optimization performance.

A. Walrus Optimizer

The WO is a metaheuristic algorithm that was recently developed and is inspired by the distinctive biological and social behaviors of walruses, the largest pinnipeds in the world,

except whales. Walruses are amphibious and gregarious creatures that inhabit temperate and Arctic waters. They are known to form groups of dozens to thousands of individuals. Their survival in challenging environments is facilitated by their distinctive morphology, which includes robust cylindrical bodies, highly sensitive vibrissae (whiskers) for tactile foraging, and continuously developing tusks. Tusks are employed for a variety of purposes, including self-defense, substrate excavation for prey, such as clams and crabs, and assistance in ascending onto ice sheets. Walruses are remarkably agile underwater, despite their massive build. They are capable of diving to depths of 500 m for up to 20 min and, in some instances, remaining submerged for 2 h before surfacing in as little as 3 min.

WO is influenced by the following key walrus behaviors:

- Breeding territoriality, where the dominant males secure prime coastal sites, proportional to the number of females in their harem.
- Acoustic-based foraging and cooperative communication, which enable survival in deep and lightless waters, where vision is limited.
- Collective defense strategies, where individuals coordinate to protect against predators, such as killer whales, including aiding injured group members.

These behaviors serve as the conceptual underpinnings of WO's search dynamics, which replicate migration, reproducing, roosting, foraging, and defensive cooperation. The algorithm is predicated on the assumption that walrus populations adjust their behavior in response to environmental cues, which are represented as "danger" and "safety" signals. It also integrates role differentiation among males, females, and juveniles to improve adaptability and diversity during optimization operations.

A multidimensional domain is characterized as the search space in the mathematical formulation of WO, which is defined by the decision variables of the problem. Each walrus is a potential solution, and its position in the search space corresponds to a potential configuration of variable values. The goal of WO is to traverse this space to identify the global optimum, which is the solution that maximizes or minimizes the objective function. Social hierarchy and behavior-inspired operators direct the population's dynamic interactions, which involve the equilibrium of exploration (global search) and exploitation (local refinement). This structure allows WO to transition between extensive exploration in uncertain "danger" conditions and focused exploitation in "safe" conditions in an adaptive manner, which is consistent with the natural survival strategies of walrus herds [17, 18].

B. Chaotic Mechanisms in Metaheuristics

The chaos theory provides deterministic, yet intricate sequences that are ergodic, non-repetitive, and highly susceptible to initial conditions. These attributes render chaotic maps a valuable addition to metaheuristic algorithms, providing an alternative to purely random number generators. Metaheuristics can achieve a more comprehensive coverage of the search space, reduce premature convergence, and maintain population diversity throughout the optimization process by utilizing chaotic sequences to replace or supplement stochastic parameters, such as initialization values, control coefficients, or position updates. Due to their adaptability and robust chaotic properties, the Logistic map, Chebyshev map, and ICMIC are among the most effective chaotic systems [19].

The Logistic map is a chaotic generator that is widely used, generating sequences that are highly sensitive and evenly distributed. These sequences have the potential to enhance both exploration and exploitation. The Chebyshev map is effective in assuring that the search space is broadly and uniformly covered during initialization or early-stage exploration, as it generates values with strong ergodicity. Sequences that combine intermittent large jumps with fine local variations are produced by the ICMIC, which exhibits a distinctive pattern of repeated collapses. This distinctive behavior is essential for the prevention of stagnation in local optima, as it facilitates a seamless transition between the intensification and diversification periods [20].

Upon integration into metaheuristics, these chaotic maps introduce deterministic, yet unpredictable variations that enhance the balance between global search and local refinement and improve convergence reliability [21]. In a variety of unimodal and multimodal optimization problems, empirical studies have demonstrated that such integration can result in enhanced consistency, higher success rates in reaching global optima, and faster convergence.

III. CHAOTIC-ENHANCED WALRUS OPTIMIZER

The proposed CWO combines the social behavior–inspired search strategy of WO with the diversity-enhancing capabilities of chaotic maps. The Logistic, Chebyshev, and ICMIC maps are integrated into the WO process at critical phases, such as population initialization, control parameter adaptation, and movement updates, in this hybrid approach. The hybrid seeks to realize a more dynamic equilibrium between exploration and exploitation by substituting conventional random values with deterministic yet indeterminate chaotic sequences. Adaptive, non-repetitive perturbations are introduced in later stages to refine promising solutions, and the chaotic components assure broader search space coverage during early iterations. The objective of this synergy between chaos-driven variability and biologically inspired operators of WO is to enhance the algorithm's robustness, maintain solution diversity, and accelerate convergence across a diverse array of intricate optimization problems.

A. Chaotic Map Integration

Although standard WO exhibits robust exploration and exploitation, it may still experience premature convergence or a loss of diversity in subsequent iterations. In order to overcome these obstacles, the proposed CWO incorporates deterministic chaotic maps to supplant the purely random components in the initialization, parameter adaptation, and position updates of the WO. The chaos theory generates sequences that are ergodic, extremely sensitive to initial conditions, and non-repetitive—characteristics that enhance search space coverage and mitigate stagnation. Three chaotic maps are integrated:

- Logistic Map: This map generates sequences that are both extremely sensitive and simple, thereby enhancing the search's convergence and diversity properties [16].
- Chebyshev Map– It produces sequences that are highly ergodic, which ensures that the search space is uniformly covered and facilitates exploration during initialization and migration.
- ICMIC– This map incorporates fine-grained variations with large-scale leaps to facilitate adaptive transitions between exploration and exploitation.

In CWO, these maps are utilized to generate non-repetitive adaptive updates by replacing random coefficients in migration, breeding, and foraging formulas; to chaotically initialize walrus positions to enhance diversity; and to dynamically balance exploration and exploitation throughout the run by modulating control parameters.

B. Detailed Description of the Proposed CWO Method

The proposed CWO follows the original WO structure but replaces stochastic elements with chaotic sequences generated by the Logistic, Chebyshev, or ICMIC. This integration improves ergodicity, prevents repetitive patterns, and enhances both exploration and exploitation.

1) Initialization

In the original WO, the initial population (X) is generated using uniform random numbers:

$$X = LB + rand(UB - LB) \quad (1)$$

In CWO, the rand term is replaced by chaotic sequences from one of the three maps:

$$\text{Logistic: } x_{i+1} = ax_i(1 - x_i) \quad (2)$$

$$\text{Chebyshev: } x_{k+1} = \cos\left(kcos^{-1}(x_k)\right) \quad (3)$$

$$\text{ICMIC: } x_{i+1} = sin\left(\frac{a\pi}{x_i}\right) \quad (4)$$

The chaotic sequence is normalized to (0, 1) where necessary, then used in (1) to produce an evenly dispersed and ergodic initial population.

2) Danger and Safety Signals

Walruses are very vigilant, both in foraging and roosting. There are 1 to 2 walruses as guards patrolling around, and danger signals are sent out immediately once unexpected situations are found. The danger signal and safety signal in WO are defined as:

$$Danger_{signal} = A \times R \quad (5)$$

$$\alpha = 1 - t/T \quad (6)$$

$$A = 2 \times \alpha \quad (7)$$

$$R = 2 \times r_1 - 1 \quad (8)$$

where A and R are danger factors, α decreases from 1 to 0 with the number of iterations t, and T is the maximum iteration. The safety signal corresponding to the danger signal in WO is defined as:

$$Safety_{signal} = r_2 \quad (9)$$

where, r_1 and r_2 are random numbers in the range of (0, 1).

3) Migration (Exploration)

When risk factors become too high, walrus herds migrate to areas more suitable for population survival. In this phase, the walrus position is updated as:

$$X_{i,j}^{t+1} = X_{i,j}^{t} + Migration\_step \quad (10)$$

$$Migration_{step} = (X_m^t - X_n^t) \times \beta \times r_3^2 \quad (11)$$

$$\beta = 1 - \frac{1}{1+\exp\left(-\frac{t-\frac{T}{2}}{T}\times 10\right)} \quad (12)$$

where $X_{i,j}^{t+1}$ is the new position for the i^{th} walrus on the j^{th} dimension, $X_{i,j}^{t}$ is the current position of the i^{th} walrus on the j^{th} dimension, $Migration_{step}$ is the step size of walrus movement. Two vigilantes are randomly selected from the population, and the positions of the vigilantes correspond to X_m^t and X_n^t, β is the migration step control factor, which varies with iteration as a smooth curve, and r_3^2 is a random number in the range of (0, 1).

4) Reproduction (Exploitation)

In contrast to migration, walrus herds tend to breed in currents when the risk factors are low. During reproduction, there are mainly two behaviors: onshore roosting and underwater foraging. The mathematical model is:

a) Roosting Behavior

The male, female, and juvenile walruses represent the classification of population members. They have different ways of renewing their position.

- Step 1: Redistribution of male walruses: The population diversity is crucial to the later iterative search for superiority. In the quasi-Monte Carlo method, the Halton sequence is a widely used method to generate randomly distributed sequences. Adopting the Halton sequence distribution for male walrus position update can allow a broader distribution of the population within the search space. The principle is to divide the search area evenly into several parts and select a random point in each part. This ensures both randomness and uniformity.
- Step 2: Position update of female walruses: The female walrus is influenced by the male walrus $Male_{i,j}^t$ and the lead walrus X_{best}^t as the process of iteration. The female walrus becomes gradually less influenced by the mate and more by the leader:

$$Female_{i,j}^{t+1} = Female_{i,j}^{t} + \alpha\left(Male_{i,j}^{t} - Female_{i,j}^{t}\right) + (1-\alpha)\left(X_{best}^{t} - Female_{i,j}^{t}\right) \quad (13)$$

where $Female_{i,j}^{t+1}$ is the new position for the i^{th} female walrus on the j^{th} dimension, $Male_{i,j}^t$ and $Female_{i,j}^t$ are the positions of the i^{th} male and female walruses on the j^{th} dimension.

- Step 3: Position update of juvenile walruses: Juvenile walruses at the edge of the population are often targeted by

killer whales and polar bears. Therefore, juvenile walruses need to update their current position to avoid predation:

$$Juvenile_{i,j}^{t+1} = \left(O - Juvenile_{i,j}^{t}\right)P \quad (14)$$

$$O = X_{best}^{t} + Juvenile_{i,j}^{t} \times LF \quad (15)$$

where $Juvenile_{i,j}^{t+1}$ is the new position for the i^{th} juvenile walrus on the j^{th} dimension, $Juvenile_{i,j}^{t}$ is the position of the i^{th} juvenile walrus on the j^{th} dimension, P is the distress coefficient of the juvenile walrus, and is a random number in (0, 1), O is the reference safety position, and LF is a vector of random numbers based on the Levy distribution representing the Levy movement:

$$Levy(a) = 0.05 \times \frac{x}{|y|^{\frac{1}{a}}} \quad (16)$$

where x and y are two normally distributed variables, $x\ N(0, \sigma_x^2)$, $y\ N(0, \sigma_y^2)$.

$$\sigma_x = \left[\frac{\Gamma(1+\alpha)sin\left(\frac{\pi\alpha}{2}\right)}{\Gamma\left(\frac{1+\alpha}{2}\right)\alpha 2^{\frac{(\alpha-1)}{2}}}\right]^{\frac{1}{\alpha}}, \sigma_y = 1, \alpha = 1.5 \quad (17)$$

where σ_x and σ_y are the standard deviations.

b) Foraging Behavior

Underwater foraging includes fleeing and gathering behaviors.

1. Fleeing Behavior

Walruses are also attacked by natural predators during underwater foraging, and they will flee from their current activity area based on danger signals from their peers. This behavior occurs in the late iteration of the WO, and a certain degree of perturbation to the population helps walruses to conduct global exploration.

$$X_{i,j}^{t+1} = X_{i,j}^{t} \cdot R - \left|X_{best}^{t} - X_{i,j}^{t}\right| \cdot r_4^2 \quad (18)$$

where $|X_{best}^{t} - X_{i,j}^{t}|$denotes the distance between the current walrus and the best walrus, and r_4 is a random number in the range of (0, 1).

2. Gathering Behavior

Walruses can cooperate to forage and move according to the location of other walruses in the population, and sharing location information can help the whole walrus herd to find the sea area with higher food abundance.

$$X_{i,j}^{t+1} = \frac{(X_1 + X_2)}{2} \quad (19)$$

$$\begin{cases} X_1 = X_{best}^{t} - a_1 \times b_1 \times \left|X_{best}^{t} - X_{i,j}^{t}\right| \\ X_2 = X_{second}^{t} - a_2 \times b_2 \times \left|X_{second}^{t} - X_{i,j}^{t}\right| \end{cases} \quad (20)$$

$$a = \beta \times r_5 - \beta \quad (21)$$

$$b = \tan(\theta) \quad (22)$$

where X_1 and X_2 are two weights affecting the gathering behavior of walrus, $X_{second}^{t}$is the position of the second walrus in the current iteration, $|X_{second}^{t} - X_{i,j}^{t}|$ denotes the distance between the current walrus and the second walrus, a and b are the gathering coefficients, r_5 is a random number in the range of (0, 1), and θ has values between 0 to π.

C. Algorithmic Flow

The CWO follows the same loop structure as the original WO, but all stochastic variables ($rand, r_1, r_2, r_3, r_4, r_5, P, x, y$) are replaced with chaos-derived sequences. The chaotic map can be switched depending on problem characteristics, and map parameters (e.g., a in Logistic/ICMIC) can be tuned for specific optimization tasks.

To further elucidate the applicability of the proposed CWO, consider its use in the surface roughness minimization problem should be considered. In this instance, the decision variables are the depth of cut, input rate, and cutting speed, all of which are subject to machining constraints. The chaotic initialization of walrus populations by the CWO is initiated by the use of ICMIC, Chebyshev, or Logistic maps to improve the diversity of the search. Chaotic sequences supplant random values during migration and foraging phases, ensuring the balanced exploration and exploitation of feasible solutions. The algorithm then iteratively updates positions until convergence, evaluating each candidate solution using the surface roughness equation as the objective function. This example demonstrates the practical application of the CWO to optimize machining parameters, thereby minimizing surface roughness while maintaining computational efficiency.

D. Computational Complexity

When solving optimization problems, the computational complexity is very useful to evaluate the efficiency of an algorithm, which depends on three main processes: initialization, fitness evaluation, and updating of the solution. The computational complexity of the initialization process and the updating mechanism are $O(N)$ and:

$$O(N \times T) + O(N \times T \times D)$$

where N is the population size, T are the maximum iterations, and D is the dimension of the given problem. Therefore, the computational complexity of WO is given by:

$$O(N \times (T + T \times D + 1))$$

The space complexity of the WO algorithm is the maximum amount of space used at any one time, which is considered during its initialization process. Thus, the space complexity of the WO algorithm is $O(N \times Dim)$.

IV. RESULTS AND DISCUSSION

In order to assess the algorithmic performance, the preliminary study implemented eight canonical no-noise benchmark test functions: Branin, Camelback, Goldstein–Price, Parabolic, Rastrigin, Rosenbrock, Shekel, and Styblinski. The diverse landscapes of these functions, which range from simple convex parabolic forms to highly multimodal surfaces with multiple local optima, make them widely used in optimization research. The incorporation of both unimodal and multimodal functions enables a fair evaluation of the exploration and exploitation capabilities of the algorithms that have been tested. The WO and its hybridization variants involve only a few

algorithm-specific control parameters, with population size and the number of iterations being the primary factor. This simplicity facilitates ease of implementation. In the present study, 5,000 iterations with 20 independent runs were employed for the non-constrained problems, whereas 20,000 iterations with 20 independent runs were applied to the machining problems. All experiments were conducted using Visual C#.

The statistical measures of average, minimum, maximum, and standard deviation values across multiple trials summarize the results, and indicate that the performance is stable and competitive. For example, the Parabolic and Rosenbrock functions consistently produced results that were near-optimal with minimal deviations, demonstrating their ability to effectively address unimodal problems. In contrast, the algorithms' sensitivity to local optima was evident in the more complex multimodal functions, such as Rastrigin and Camelback, which exhibited a larger degree of variation. It is important to note that the chaos-enhanced variants of Logistic, Chebyshev, and ICMIC (CWO1–CWO3) frequently exhibited reduced variance in comparison to the baseline WO, particularly in the Styblinski and Shekel functions. This suggests that the variants have improved convergence stability and reliability in preventing premature stagnation. The results of the experiments on the eight functions with no noise on the response are presented in Table I.

The proposed chaos-embedded metaheuristic algorithms were further extended to a series of benchmark machining optimization problems, resulting in computational results and performance analyses. The optimization of the machining parameters is of paramount importance in contemporary manufacturing, as it has a direct impact on product quality, operational cost, tool life, and overall productivity. The necessity of comprehensive optimization strategies is underscored by the substantial differences in energy consumption, tool wear, and surface integrity that can result from minor changes in cutting speed, feed rate, or depth of cut.

The chosen machining models are designed to achieve a variety of objectives, which are frequently in conflict. These objectives include the reduction of production costs to enhance economic competitiveness, the optimization of MRR to improve productivity, and the reduction of surface imperfections to improve product quality [22]. The problem space is highly non-linear and multi-variable due to the realistic industrial limitations that constrain these objectives, including allowable cutting forces, spindle power, tool life, and thermal thresholds [23, 24]. The trade-offs that are frequently encountered in practical machining environments are reflected in each model, which represents a unique optimization challenge.

In order to tackle these obstacles, chaos-embedded metaheuristics are implemented to preserve a dynamic equilibrium between exploration and exploitation, thereby minimizing the likelihood of premature convergence and improving the dependability of the solutions that are obtained. Ergodicity and non-repetitive search patterns are introduced by the integration of chaotic dynamics, which enhances solution diversity and expedites convergence toward high-quality optima. The proposed algorithms' performance and robustness are assessed based on the four benchmark machining problem formulations, which include surface roughness minimization, MRR maximization, multi-pass turning cost minimization, and integrated multi-pass optimization, as examined in this study.

TABLE I. RESULTS OF EXPERIMENTS ON EIGHT FUNCTIONS WITH NO NOISE ON THE RESPONSE

Branin Function				
Index	WO	CWO1	CWO2	CWO3
Average	5.365	5.354	5.357	5.369
Min	5.174	5.174	5.169	5.261
Max	5.400	5.400	5.400	5.400
SD	0.064	0.067	0.067	0.045
Camelback Function				
Index	WO	CWO1	CWO2	CWO3
Average	36.436	37.574	37.879	38.000
Min	33.238	33.687	33.499	32.897
Max	39.942	41.802	40.859	40.972
SD	1.977	2.349	2.160	2.151
Goldstein-Price Function				
Index	WO	CWO1	CWO2	CWO3
Average	8.317	8.511	8.423	8.711
Min	7.603	7.686	7.873	8.013
Max	8.912	9.442	9.339	9.511
SD	0.338	0.491	0.379	0.400
Parabolic Function				
Index	WO	CWO1	CWO2	CWO3
Average	11.998	11.999	11.998	11.999
Min	11.991	11.995	11.984	11.996
Max	12.000	12.000	12.000	12.000
SD	0.002	0.001	0.004	0.001
Rastrigin Function				
Index	WO	CWO1	CWO2	CWO3
Average	97.150	97.148	98.427	98.157
Min	91.445	91.705	95.094	95.504
Max	99.926	99.984	99.997	99.997
SD	2.361	2.237	1.688	1.733
Rosenbrock Function				
Index	WO	CWO1	CWO2	CWO3
Average	79.998	79.997	79.999	79.999
Min	79.986	79.988	79.992	79.993
Max	80.000	80.000	80.000	80.000
SD	0.004	0.003	0.002	0.002
Shekel Function				
Index	WO	CWO1	CWO2	CWO3
Average	18.731	18.980	18.980	18.981
Min	13.982	18.980	18.980	18.980
Max	18.981	18.981	18.981	18.981
SD	1.118	0.000	0.000	0.000
Styblinski Function				
Index	WO	CWO1	CWO2	CWO3
Average	352.763	352.888	353.145	353.159
Min	351.275	351.530	352.525	352.636
Max	353.328	353.316	353.330	353.332
SD	0.571	0.464	0.182	0.169

SD is short for Standard Deviation.

A. Turning Surface Roughness Minimization Model

Authors in [7] investigated the effects of cutting parameters on surface roughness in the turning of OHNS steel, a material widely used in die-making and tooling applications due to its hardness and dimensional stability. Surface roughness was selected as the primary response variable because it directly

influences product quality, functional performance, and post-processing requirements. To quantify this relationship, a multiple linear regression model was developed that links surface roughness R_a with three key cutting parameters: cutting speed, feed rate, and depth of cut. This model allows prediction of surface finish under different machining conditions and provides a mathematical basis for parameter optimization in turning operations. The mathematical model is defined as:

Minimize:

$$R_a = 8.11 - 0.0217 \cdot A - 25.9 \cdot B - 6.37 \cdot C + 0.0563 \cdot AC + 19.4 \cdot BC \quad (23)$$

Subject to:

$150 \leq A \leq 250$ (m/min)

$0.1 \leq B \leq 0.2$ (mm/rev)

$0.5 \leq C \leq 1.5$ (mm)

where A is the cutting speed (m/min), B is the feed rate (mm/rev), C is the depth of cut (mm), and R_a is the surface roughness (µm).

B. Turning MRR Maximization Model

Authors in [8] performed a series of controlled turning experiments on mild steel to investigate the influence of the key cutting parameters on machining performance. Spindle speed, cutting speed, and feed rate were systematically varied across multiple levels to evaluate their combined effect on the MRR, a critical indicator of machining productivity. The findings highlighted the sensitivity of MRR to parameter selection, emphasizing the importance of optimizing these variables to achieve higher efficiency without compromising tool life or surface quality. Based on their experimental observations, the following mathematical model was developed to describe and quantify the relationship between the machining parameters and MRR:

Maximize:

$$MRR = 1.42 - 1.83 \cdot A - 0.9 \cdot B + 10 \cdot C + 103 \cdot AB - 112 \cdot AC + 0.000014BC \quad (24)$$

Subject to:

$0.62 \leq A \leq 0.98$ (mm/rev)

$40 \leq B \leq 1000$ (rpm)

$3.5 \leq C \leq 95.5$ (m/min)

where A is the feed rate (mm/rev), B is the spindle speed (rpm), and C is the cutting speed (m/min).

C. Multi-Pass Turning Cost Minimization

Authors in [25] proposed a comprehensive multi-pass turning optimization model (IVATA) for machining mild steel with a carbide cutting tool, and the primary objective of minimizing production cost expressed in dollars per piece. The model integrates multiple machining constraints, including cutting speed limits, allowable feed rates, depth of cut ranges, cutting force, spindle power, tool life, and thermal restrictions, making it highly representative of real industrial conditions. By accounting for both economic and technological factors, the formulation captures the trade-offs between productivity, tool wear, and process stability. The mathematical model governing this multi-pass turning cost minimization problem is defined as:

$$Min.Cost = n(1341.59V^{-1}f^{-1}d^{-4} + 2.879 \times 10^{-8}V^4 f^{0.75}d^{-0.025} + 10)$$

Subject to:

$50 \leq V \leq 400$ (m/min):

$0.30 \leq f \leq 0.75$ (mm/rev):

$1.20 \leq d \leq 2.75$ (mm):

$Cutting\ force\ (F_c) \leq 8.5$ (kg):

where:

$$F_c = (28.10V^{0.07} - 0.525V^{0.5})d \times f\left(1.59 + 0.946\frac{(1+x)}{\sqrt{(1-x)^2+x}}\right)$$

$$x = \left(\frac{V}{142}exp(2.21f)\right)^2$$

Cutting power:

$$(P_c) = \frac{0.746F_cV}{4500}$$

$P_c \leq 2.25$ kW

with:

$$\text{Tool life } (TL) = 60\left(\frac{10^{10}}{V^5 f^{1.75} d^{0.75}}\right)$$

$$\text{Temperature } (T) = 132V^{0.4}f^{0.2}d^{0.105}$$

$25 \leq TL \leq 45$ min

$T \leq 1000$

The limitations on the value of the depth of cut in removing A in n passes are given by $\frac{A}{d} = n$.

D. Integrated Multi-Pass Turning Model

The integrated multi-pass turning model is designed to simultaneously optimize multiple machining performance measures by considering the trade-offs between machining time, production cost, and surface roughness within a unified framework. Unlike single-objective models, this formulation employs a nonlinear objective function that aggregates key responses into a composite performance index Z. Such an approach is particularly relevant in real-world manufacturing, where productivity, cost-effectiveness, and quality must be balanced under stringent industrial constraints. This model jointly optimizes unit machining time through a nonlinear objective function. The mathematical model is defined as:

$$Z(T_P, C_P, R_a) = 0.42e^{(-0.22T_P)} + 0.36e^{(-0.32C_P)} + 0.17e^{(-0.26R_a)} + 0.05/(1 + 1.22T_PC_PR_a) \quad (25)$$

$$MinC_P = (13.55/T + 0.39)TP$$

$$MinR_a = 0.0088v + 0.3232f + 0.3144a$$

Subject to:

$$T = 1575134.21(v^{-1.7} f^{-1.55} a^{-1.22})$$

$$MRR = 1000vfa$$

$$70 \le v \le 90, 0.1 \le f \le 2, 0.1 \le a \le 5$$

$$0.000626(vf^{1.18}a^{1.26}) \le 5, 1.38(f^{1.18}a^{1.26}) \le 230$$

The results in Table II indicate a clear improvement in minimizing surface roughness when chaos-enhanced algorithms are applied. The baseline WO algorithm achieved an average roughness of 0.0256 µm with a relatively large variation (SD = 0.0421). In contrast, the chaotic variants CWO1, CWO2, and especially CWO3 consistently yielded lower averages, with CWO3 reaching 0.0126 µm and the lowest standard deviation of 0.0247. This demonstrates that the chaotic enhancements significantly improved both solution quality and stability. The maximum surface roughness values further confirm this trend, where CWO3 limited the worst-case outcome to 0.1101 µm compared to 0.1672 µm in WO. These results suggest that introducing chaos mechanisms enhances the algorithm's ability to avoid suboptimal regions and converge to smoother, more reliable turning conditions.

TABLE II. RESULTS OF EXPERIMENTS ON THE TURNING SURFACE ROUGHNESS MINIMIZATION MODEL

Index	WO	CWO1	CWO2	CWO3
Average	0.0256	0.0199	0.0153	0.0126
Min	0.0030	0.0008	0.0012	0.0002
Max	0.1672	0.1584	0.1584	0.1101
SD	0.0421	0.0408	0.0349	0.0247

For the MRR maximization model, presented in Table III, all algorithms performed well, achieving values close to the theoretical upper bound. The baseline WO recorded an average of 99,593 mm³/min, whereas the chaotic variants showed incremental improvements, with CWO3 reaching the highest average (99,628 mm³/min) and the lowest variation (SD = 43.85). Although the performance differences are subtle due to the problem's less complex nature, the results highlight the role of chaotic strategies in fine-tuning search precision. CWO3 in particular provided not only the highest average but also the narrowest spread between minimum and maximum values, indicating better convergence stability and robustness against parameter sensitivity.

The results for the cost minimization problem, displayed in Table IV, reveal that all algorithms converged to highly similar solutions, with average costs around $96 per piece. However, the chaotic variants again demonstrated a marginal edge in terms of stability. CWO2 produced the lowest average cost (96.020) and one of the narrowest standard deviations (0.038), while CWO3 achieved the smallest variability overall (SD = 0.026). These small but consistent improvements suggest that while the cost function is relatively smooth and less multimodal, the integration of chaos dynamics contributes to more reliable convergence, ensuring minimal deviations from the optimal cost under repeated runs.

The integrated model, depicted in Table V, evaluated multiple performance criteria simultaneously, including machining time and MRR. The results show that all algorithms converged to nearly identical solutions, with negligible differences in the aggregated objective value Z (all ≈ 0.8186). Closer inspection reveals slight distinctions: CWO2 achieved the highest MRR (991,466 mm^3/min) and shortest machining time (30.478 min), while CWO1 yielded the lowest production cost ($0.3294). Meanwhile, WO and CWO3 provided balanced trade-offs across all parameters. These outcomes illustrate that chaos-enhanced variants can shift optimization emphasis slightly, offering flexibility depending on whether productivity, cost, or quality is prioritized. Overall, the results confirm the reliability of both standard and chaotic algorithms, with the chaotic variants offering marginal yet valuable improvements in efficiency and solution diversity.

TABLE III. RESULTS OF EXPERIMENTS ON THE TURNING MRR MAXIMIZATION MODEL

Index	WO	CWO1	CWO2	CWO3
Average	99593.2247	99612.1178	99599.3913	99627.8227
Min	99344.1442	99439.8839	99417.3002	99526.4768
Max	99672.1112	99674.1890	99682.3541	99684.7977
SD	70.7559652	58.7494165	58.8502127	43.8454244

TABLE IV. RESULTS OF EXPERIMENTS ON THE MULTI-PASS TURNING COST MINIMIZATION

Index	WO	CWO1	CWO2	CWO3
Average	96.033	96.021	96.020	96.022
Min	96.005	96.005	96.005	96.005
Max	96.134	96.162	96.163	96.095
SD	0.041	0.039	0.038	0.026

TABLE V. COMPARISON OF THE BEST OPTIMAL SOLUTIONS OF INTEGRATED MULTI-PASS TURNING MODEL

Parameter	WO	CWO1	CWO2	CWO3
v (mm/min)	99.8359	99.333	99.515	99.671
f (mm/rev)	1.9931	1.9850	1.9936	1.9862
a (mm)	4.9741	4.9996	4.9975	4.9955
T_P (min)	0.3958	0.3967	0.3954	0.3960
C_P ($)	0.3302	0.3294	0.3300	0.3298
R_a (µm)	3.0866	3.0876	3.0913	3.0896
MRR (mm^3/min)	989765.6	985815.7	991466.5	988915.5
T (min)	30.4977	30.762	30.478	30.589
F (N)	23.5064	23.545	23.653	23.537
P (kw)	0.0880	0.0875	0.0877	0.0878
Z	0.8186	0.8186	0.8186	0.8185

The comparative performance of the WO and its chaotic variants (CWO1–CWO3) was assessed across both classical test functions and machining optimization models. The numerical results presented in Tables I-IV and the graphical illustrations in Figures 1-3 provide complementary insights into the advantages and trade-offs associated with the integration of chaos theory.

For the surface roughness minimization model, the convergence chart, as shown in Figure 3, demonstrates a significant advantage of the chaotic variants over the baseline WO. WO exhibits a gradual decline, requiring nearly 800 iterations to reach near-optimal regions, whereas CWO2 and CWO3 converge rapidly within the first 200 iterations. The statistical results in Table I confirm this trend, with CWO3

producing the lowest average roughness (0.0126 µm) and the smallest standard deviation (0.0247). This shows that chaotic integration enhances not only convergence speed but also solution stability, a crucial factor in machining environments where precision is required.

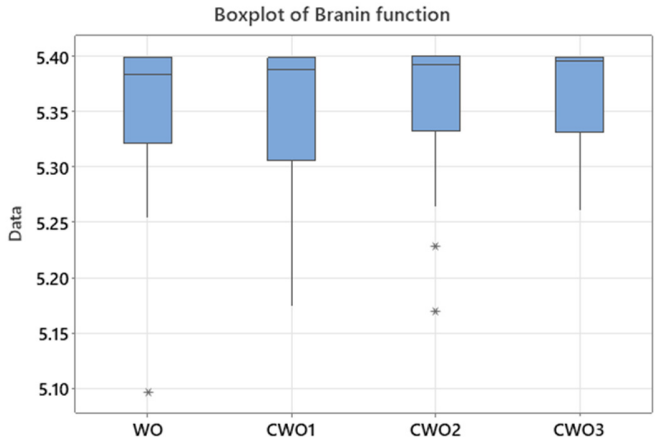

Fig. 1. Comparative boxplot results of WO and its chaotic variants (CWO1–CWO3) on the Branin benchmark function.

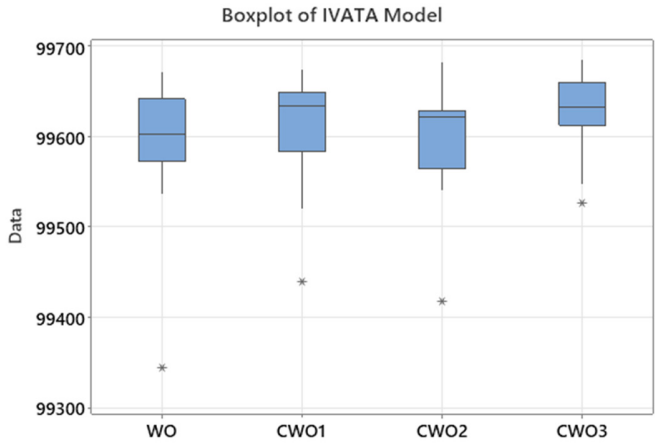

Fig. 2. Comparative boxplot results of WO and its chaotic variants (CWO1–CWO3) on the IVATA model.

The MRR maximization model further highlights these improvements. As illustrated in Table II, all algorithms achieve near-optimal values, but CWO3 records the highest average MRR (99,627 mm³/min) with the lowest variability. The boxplot of the IVATA model, as shown in Figure 2, reinforces this result, where CWO3 displays the most compact distribution of outcomes and fewer outliers compared to WO. This indicates that chaos-enhanced variants reduce fluctuations and ensure more reliable convergence in production-focused optimization. In the multi-pass cost minimization model, the results in Table III reveal marginal differences among the algorithms, with the average costs converging to approximately $96. However, CWO3 again demonstrates the lowest variability (SD = 0.026), confirming its robustness in problems with smooth cost landscapes. Similarly, the results of the integrated multi-pass turning model, presented in Table IV, show that all methods achieve comparable performance, with aggregated objective values Z converging to ~0.8186. Minor differences exist—CWO2 achieves the highest MRR, while CWO1 slightly reduces cost—but overall, the chaotic variants improve stability and maintain the trade-offs across time, cost, and quality objectives.

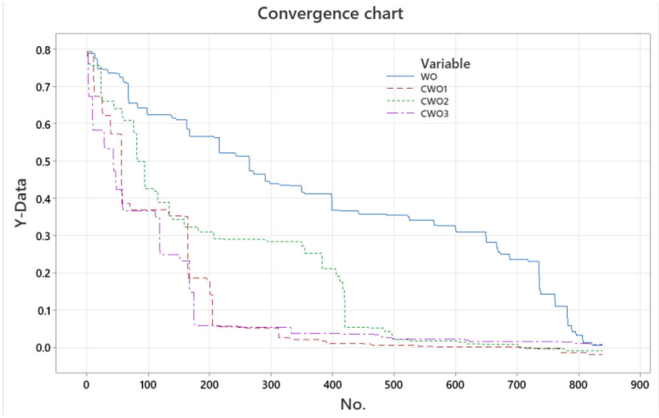

Fig. 3. Speed of convergence rate according to [7].

The boxplots of benchmark functions, as evidenced in Figure 1 for Branin and Figure 2 for IVATA, further emphasize these findings. WO consistently exhibits wider spreads and occasional low-performing outliers, suggesting greater variability in performance. In contrast, the chaotic variants, particularly CWO3, achieve tighter interquartile ranges and higher median values, signaling improved convergence reliability. Nevertheless, outliers in CWO1 and CWO2 highlight occasional instability, pointing to sensitivity in the way chaos is embedded. Overall, the results confirm that integrating chaotic dynamics into WO strengthens convergence speed, improves robustness, and reduces variability across both synthetic benchmarks and machining optimization problems. Among the variants, CWO3 emerges as the most effective, consistently delivering faster convergence and tighter solution distributions, making it the most suitable approach for complex and precision-driven machining optimization tasks.

V. CONCLUSION

This study introduced a chaos-enhanced Walrus Optimizer (WO) by embedding three chaotic maps—Logistic, Chebyshev, and Iterative Chaotic Map with Infinite Collapses (ICMIC)—into key phases of the algorithm, including initialization, migration, reproduction, and foraging. The proposed variants, WO-Logistic, WO-Chebyshev, and WO-ICMIC, were evaluated on four machining optimization problems: (1) surface roughness minimization, (2) Material Removal Rate (MRR) maximization, (3) multi-pass turning cost minimization, and (4) a multi-objective model integrating time, cost, and roughness. The comparative analysis against the standard WO and several state-of-the-art metaheuristics demonstrated that the chaos-enhanced versions achieved superior performance in terms of solution accuracy, convergence speed, and stability. These findings confirm that integrating chaotic maps provides a robust and effective

framework for solving complex machining optimization problems.

For future research, an interesting direction is the development of an adaptive chaos embedding strategy. Instead of using fixed chaotic maps throughout the optimization process, an adaptive framework could dynamically select or tune chaotic sequences (e.g., Logistic, Chebyshev, ICMIC) based on the feedback from convergence rate, solution diversity, or performance indicators at different stages of the search. This approach would enable the optimizer to adjust its exploration–exploitation balance more effectively. Similar adaptive and self-adaptive mechanisms have been successfully applied in metaheuristic frameworks for parameter control and dynamic strategy selection, suggesting that adaptive chaos embedding could further enhance robustness and efficiency in solving complex machining optimization problems.

ACKNOWLEDGMENT

This research was funded by the Faculty of Engineering, King Mongkut's University of Technology North Bangkok (Contract No. ENG-67–005), and this study was supported by the Thammasat University Research Fund (Contract No. TUFT 110/2567)

DECLARATION OF COMPETING INTEREST

The authors declare that they have no conflict of interest.

DATA AVAILABILITY STATEMENT

The data that support the findings of this study are available from the first author (Pasura Aungkulanon) upon reasonable request.

REFERENCES

[1] K. S. Sangwan and G. Kant, "Optimization of Machining Parameters for Improving Energy Efficiency using Integrated Response Surface Methodology and Genetic Algorithm Approach," *Procedia CIRP*, vol. 61, pp. 517–522, 2017, https://doi.org/10.1016/j.procir.2016.11.162.

[2] M. Han, Z. Du, K. F. Yuen, H. Zhu, Y. Li, and Q. Yuan, "Walrus Optimizer: A Novel Nature-inspired Metaheuristic Algorithm," *Expert Systems with Applications*, vol. 239, Apr. 2024, Art. no. 122413, https://doi.org/10.1016/j.eswa.2023.122413.

[3] S. Mirjalili, A. H. Gandomi, S. Z. Mirjalili, S. Saremi, H. Faris, and S. M. Mirjalili, "Salp Swarm Algorithm: A Bio-inspired Optimizer for Engineering Design Problems," *Advances in Engineering Software*, vol. 114, pp. 163–191, Dec. 2017, https://doi.org/10.1016/j.advengsoft.2017.07.002.

[4] S. Mirjalili, S. M. Mirjalili, and A. Lewis, "Grey Wolf Optimizer," *Advances in Engineering Software*, vol. 69, pp. 46–61, Mar. 2014, https://doi.org/10.1016/j.advengsoft.2013.12.007.

[5] T. M. Shami, A. A. El-Saleh, M. Alswaitti, Q. Al-Tashi, M. A. Summakieh, and S. Mirjalili, "Particle Swarm Optimization: A Comprehensive Survey," *IEEE Access*, vol. 10, pp. 10031–10061, 2022, https://doi.org/10.1109/ACCESS.2022.3142859.

[6] T. V. Dua, H. X. Thinh, N. C. Bao, D. V. Duc, and T. M. Hoang, "Multi-objective Optimization of the Turning Process using the Probability Method," *Engineering, Technology and Applied Science Research*, vol. 15, no. 1, pp. 19865–19870, Feb. 2025, https://doi.org/10.48084/etasr.9472.

[7] V. B. Pansare and M. V. Kavade, "Optimization of Cutting Parameters in Multipass Turning Operation using Ant Colony Algorithm," *International Journal of Engineering Science and Advanced Technology*, vol. 2, no. 4, pp. 955–960, Jul. 2012.

[8] I. Shivakoti, S. Diyaley, G. Kibria, and B. B. Pradhan, "Analysis of Material Removal Rate using Genetic Algorithm Approach," *International Journal of Scientific and Engineering Research*, vol. 3, no. 5, pp. 1–6, May 2012.

[9] K.-M. Lee, M.-R. Hsu, J.-H. Chou, and C.-Y. Guo, "Improved Differential Evolution Approach for Optimization of Surface Grinding Process," *Expert Systems with Applications*, vol. 38, no. 5, pp. 5680–5686, May 2011, https://doi.org/10.1016/j.eswa.2010.10.067.

[10] M.-C. Chen and D.-M. Tsai, "A Simulated Annealing Approach for Optimization of Multi-pass Turning Operations," *International Journal of Production Research*, vol. 34, no. 10, pp. 2803–2825, Oct. 1996, https://doi.org/10.1080/00207549608905060.

[11] Z. G. Wang, M. Rahman, Y. S. Wong, and J. Sun, "Optimization of Multi-pass Milling using Parallel Genetic Algorithm And Parallel Genetic Simulated Annealing," *International Journal of Machine Tools and Manufacture*, vol. 45, no. 15, pp. 1726–1734, Dec. 2005, https://doi.org/10.1016/j.ijmachtools.2005.03.009.

[12] G. Atali, İh. PehliVan, B. GüreviN, and H. İb. Şeker, "Chaos In Metaheuristic Based Artificial Intelligence Algorithms: A Short Review," *Turkish Journal of Electrical Engineering and Computer Sciences*, vol. 29, no. 3, pp. 1354–1367, May 2021, https://doi.org/10.3906/elk-2102-5.

[13] B. S. Yıldız, N. Pholdee, N. Panagant, S. Bureerat, A. R. Yildiz, and S. M. Sait, "A Novel Chaotic Henry Gas Solubility Optimization Algorithm for Solving Real-world Engineering Problems," *Engineering with Computers*, vol. 38, no. S2, pp. 871–883, Jun. 2022, https://doi.org/10.1007/s00366-020-01268-5.

[14] S. Kumar *et al.*, "Chaotic Marine Predators Algorithm for Global Optimization of Real-world Engineering Problems," *Knowledge-Based Systems*, vol. 261, Feb. 2023, Art. no. 110192, https://doi.org/10.1016/j.knosys.2022.110192.

[15] M. W. Ouertani, G. Manita, and O. Korbaa, "Chaotic Lightning Search Algorithm," *Soft Computing*, vol. 25, no. 3, pp. 2039–2055, Feb. 2021, https://doi.org/10.1007/s00500-020-05273-0.

[16] A. Kaveh and H. Yousefpoor, "Chaotic Optimization of Trusses with Frequency Constraints with Three Metaheuristic Algorithms," *Iranian Journal of Science and Technology, Transactions of Civil Engineering*, vol. 48, no. 1, pp. 271–293, Feb. 2024, https://doi.org/10.1007/s40996-023-01223-6.

[17] P. Trojovský and M. Dehghani, "A New Bio-inspired Metaheuristic Algorithm for Solving Optimization Problems Based on Walruses Behavior," *Scientific Reports*, vol. 13, no. 1, May 2023, Art. no. 8775, https://doi.org/10.1038/s41598-023-35863-5.

[18] Y. T. Bozkurt and M. Şimşek, "Channel Estimation in OFDM System using Walrus Optimization Algorithm," in *9th International Symposium on Innovative Approaches in Smart Technologies (ISAS)*, Gaziantep, Turkiye, Jun. 2025, pp. 1–6, https://doi.org/10.1109/ISAS66241.2025.11101734.

[19] R. Tang, S. Fong, and N. Dey, "Metaheuristics and Chaos Theory," in *Chaos Theory*, K. A. M. A. Naimee, Ed. London, United Kingdom: InTech, 2018.

[20] A. Limane *et al.*, "Chaos-enhanced Metaheuristics: Classification, Comparison, and Convergence Analysis," *Complex and Intelligent Systems*, vol. 11, no. 3, Mar. 2025, Art. no. 177, https://doi.org/10.1007/s40747-025-01791-2.

[21] I. Zelinka *et al.*, "Impact of Chaotic Dynamics on the Performance of Metaheuristic Optimization Algorithms: An Experimental Analysis," *Information Sciences*, vol. 587, pp. 692–719, Mar. 2022, https://doi.org/10.1016/j.ins.2021.10.076.

[22] H. Zhang, B. Buchmeister, X. Li, and R. Ojstersek, "An Efficient Metaheuristic Algorithm for Job Shop Scheduling in a Dynamic Environment," *Mathematics*, vol. 11, no. 10, May 2023, Art. no. 2336, https://doi.org/10.3390/math11102336.

[23] M. Bezoui, A. T. Almaktoom, A. Bounceur, S. M. Qaisar, and M. Chouman, "Hybrid Metaheuristics for Industry 5.0 Multi-Objective Manufacturing and Supply Chain Optimization," in *21st Learning and Technology Conference*, Jeddah, Saudi Arabia, Jan. 2024, pp. 245–249, https://doi.org/10.1109/LT60077.2024.10469011.

[24] E. Ficarella, L. Lamberti, and S. O. Degertekin, "Comparison of Three Novel Hybrid Metaheuristic Algorithms for Structural Optimization Problems," *Computers and Structures*, vol. 244, Feb. 2021, Art. no. 106395, https://doi.org/10.1016/j.compstruc.2020.106395.

[25] Z. Khan, B. Prasad, and T. Singh, "Machining Condition Optimization by Genetic Algorithms and Simulated Annealing," *Computers and Operations Research*, vol. 24, no. 7, pp. 647–657, Jul. 1997, https://doi.org/10.1016/S0305-0548(96)00077-9.